

# Stable $\pi$ Radical from a Contracted Doubly N-Confused Hexaphyrin by Double Palladium Metalation\*\*

Yutaka Hisamune, Keiichi Nishimura, Koji Isakari, Masatoshi Ishida, Shigeki Mori, Satoru Karasawa, Tatsuhisa Kato, Sangsu Lee, Dongho Kim,\* and Hiroyuki Furuta\*

**Abstract:** A contracted doubly N-confused dioxohexaphyrin derivative served as a dinucleating metal ligand for unsymmetrical coordination. The complexation of two palladium(II) cations led to the formation of  $\pi$ -radical species that were persistent in atmospheric air in the presence of moisture. Effective delocalization of an unpaired electron over the hexaphyrin backbone could contribute to the distinct chemical stability.

Expanded porphyrinoids have attracted great interest owing to their unique optical properties as well as redox non-innocence.<sup>[1]</sup> For example, the meso-aryl-substituted hexaphyrin **1**, which consists of six pyrrole rings, exhibits absorption/emission in the near-infrared (NIR) region and is a representative derivative capable of redox switching between a Hückel aromatic  $26\pi$  species and an antiaromatic (or Möbius aromatic)  $28\pi$  congener.<sup>[2]</sup> Such redox-rich  $\pi$  systems can stabilize the open-shell radical species by the use of their giant  $\pi$ -conjugated networks in some cases.<sup>[3]</sup> From the viewpoint of the coordination chemistry of expanded porphyrinoids, hexaphyrin **1** can provide two

unique “NNCC” coordination cavities to afford various dinucleating organometallic complexes with a variety of conformation owing to their inherent topological flexibility.<sup>[4]</sup> In contrast, the synthetic analogue of hexaphyrin with two N-confused pyrrole rings, namely, the doubly N-confused dioxohexaphyrin **2**, displays more versatility but with a defined conformation in metal complexation.<sup>[5]</sup> The relatively rigid “NNNO” donor environments of **2** facilitated the coordination of various divalent metals (e.g., zinc(II), copper(II)) with predictable conformations (Scheme 1).

Upon the structural modification of **1** through an “N-confusion” approach, two metal cations with different oxidation states (e.g., a combination of gold(III) and platinum(II)) were coordinated site selectively in a singly N-confused oxohexaphyrin **3**.<sup>[6]</sup> To further extend the coordination chemistry of expanded porphyrinoids, we examined the skeletal modification of **2**, which was expected to produce an unsymmetrical coordination environment, for example, by the loss of a meso methine carbon atom within the macrocycle. The contraction of the hexaphyrin skeleton would lead to an unsymmetrical dinucleating coordination environment with different cavity sizes for metal cations. Herein, we report the synthesis of a novel contracted version of doubly N-confused dioxo[26]hexaphyrin with an embedded bipyrrole unit (i.e., 5,10,15,20,25-pentakis(pentafluorophenyl)-substituted doubly N-confused dioxo[26]hexaphyrin(1.1.1.1.1.0), **4**). The dioxo[26]hexaphyrin **4** coordinated two palladium(II) atoms to produce an unprecedented stable  $\pi$ -radical complex under ambient conditions rather than a mixed-valent ( $\text{Pd}^{\text{II/III}}$ ) species.

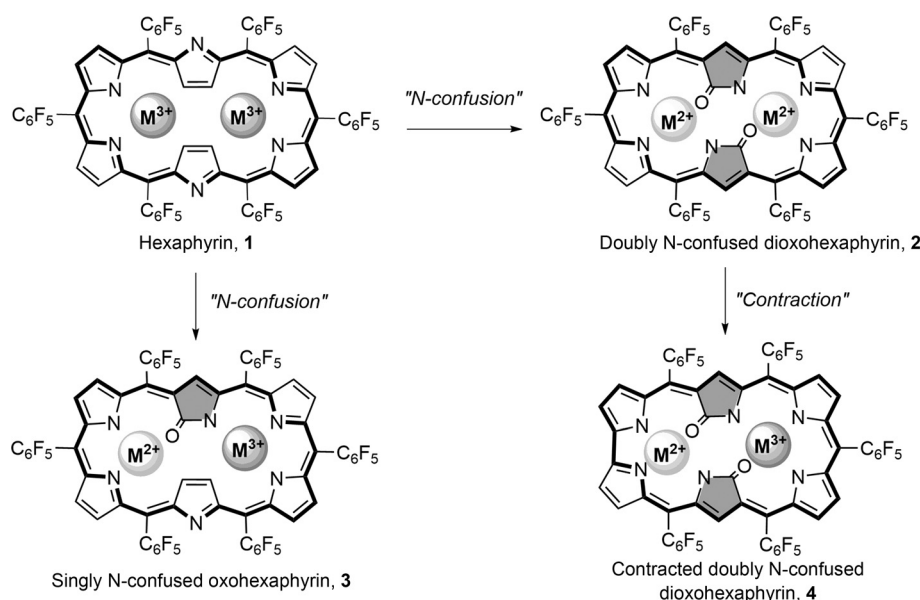
The contracted hexaphyrin analogue **4** was synthesized in a stepwise manner (Scheme 2). Regioselective monoacylation of the N-confused tripyrrane derivative **5** gave compound **6** in 40 % yield.<sup>[7]</sup> After the reduction of derivative **6** with  $\text{NaBH}_4$ , subsequent condensation with an excess amount of **5** afforded the doubly N-confused hexapyrrane precursor **7** in 61 % yield. A [6+0]-type intramolecular oxidative cyclization with 2,3-dichloro-5,6-dicyano-1,4-benzoquinone (DDQ) as the oxidant yielded the doubly N-confused [24]hexaphyrin(1.1.1.1.1.0) **8** in 18 % yield. Finally, the hexaphyrin **8** underwent reductive oxygenation with sodium dithionite in aqueous THF to give the desired doubly N-confused dioxo[26]hexaphyrin **4**.

The structure of **4** was characterized by high-resolution (HR) mass spectrometry and NMR spectroscopy (see the Supporting Information). The parent-ion peak of **4** observed at  $m/z$  1314.0917 is consistent with the proposed structure ( $[\text{M}]^+$  calcd for  $\text{C}_{59}\text{H}_{14}\text{F}_{25}\text{N}_6\text{O}_2$ : 1314.0857). The  $^1\text{H}$  NMR spectrum of **4** in  $\text{CDCl}_3$  showed the presence of three sets of

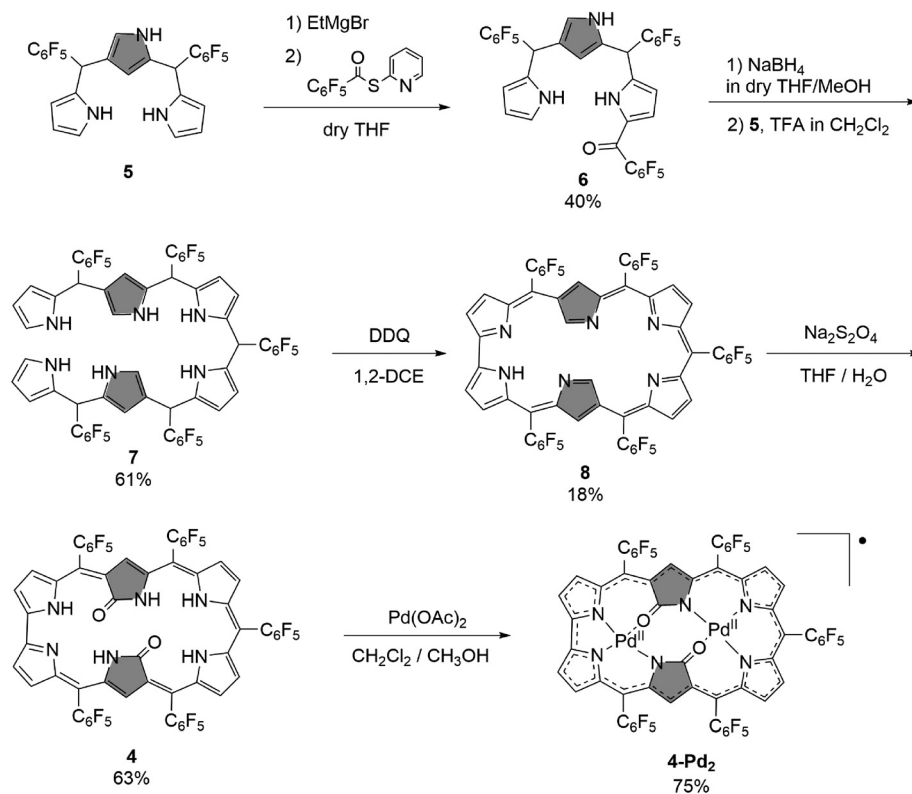
[\*] Y. Hisamune, K. Nishimura, K. Isakari, Dr. M. Ishida, Prof. Dr. H. Furuta  
Department of Chemistry and Biochemistry, Graduate School of Engineering, and Education Center for Global Leaders in Molecular Systems for Devices, Kyushu University  
Fukuoka 819-0395 (Japan)  
E-mail: hfuruta@cstf.kyushu-u.ac.jp  
Dr. S. Mori  
Integrated Center for Science, Ehime University  
Matsuyama 790-8577 (Japan)  
Prof. Dr. S. Karasawa  
Graduate School of Pharmaceutical Sciences, Kyushu University  
Fukuoka 812-8582 (Japan)  
Prof. Dr. T. Kato  
Institute for Liberal Arts and Sciences, Kyoto University  
Kyoto 606-8501 (Japan)  
S. Lee, Prof. Dr. D. Kim  
Spectroscopy Laboratory for Functional  $\pi$ -Electronic Systems and Department of Chemistry, Yonsei University  
Seoul 120-749 (Korea)  
E-mail: dongho@yonsei.ac.kr

[\*\*] We acknowledge financial support through Grants-in-Aid (25248039 to H.F. and 26810024 to M.I.) from the JSPS and by the Global Research Laboratory (2013K1A1A2A02050183 to D.K.) of the National Research Foundation of Korea (NRF), funded by the Ministry of Science, ICT (Information and Communication Technologies) and Future Planning.

Supporting information for this article is available on the WWW under <http://dx.doi.org/10.1002/anie.201502285>.



**Scheme 1.** Structural modifications of hexaphyrin skeletons for metal complexation.



**Scheme 2.** Synthesis of the contracted doubly N-confused dioxohexaphyrin bispalladium(II) complex **4-Pd<sub>2</sub>**. TFA = trifluoroacetic acid.

interior NH hydrogen atoms with high-field resonances (i.e.,  $\delta = -6.23, -2.58, -1.11$  ppm), which were assigned by a D<sub>2</sub>O-exchange experiment. The peripheral  $\beta$ -pyrrolic hydrogen atoms appeared at relatively low field around 9.3–10.8 ppm. Comparison with the spectrum of the hexaphyrin **2** led us to anticipate the rectangular-type conformation in solution.<sup>[5]</sup>

The chemical-shift difference between interior N–H atoms and exterior  $\beta$ -H atoms,  $\Delta\delta_{\text{CH-NH}}$ , was estimated to be 17.0 ppm, which suggests a stronger aromaticity as a result of the diatropicity of the 26 $\pi$ -conjugated circuit. The negative nucleus-independent chemical-shift (NICS) value calculated at the global center of the macrocycle ( $\delta = -13.3$  ppm) supports distinct aromaticity (see Figure S11 in the Supporting Information).

The UV/Vis/NIR absorption spectrum of **4** shows characteristic aromatic features: an intense Soret band split at  $\lambda_{\text{max}} = 568$  and 606 nm and well-resolved Q-like bands at 726, 792, 877, and 1000 nm (Figure 1). Fluorescence emission of **4** was observed at  $\lambda_{\text{max}} = 1010$  nm with a small Stokes shift (99 cm<sup>−1</sup>), again supporting the aromatic nature of **4** (see Figure S12).

Upon palladium complexation, the electronic properties of aromatic hexaphyrin **4** were dramatically altered. Metalation was performed by mixing a solution of **4** in CH<sub>2</sub>Cl<sub>2</sub>/MeOH with Pd(OAc)<sub>2</sub> (10 equiv) at room temperature. Silica-gel column-chromatographic separation then gave a pure green fraction of the bis-palladium complex **4-Pd<sub>2</sub>** in 75% yield. The UV/Vis/NIR absorption spectrum of the product exhibited a less intense Soret-like band at  $\lambda_{\text{max}} = 637$  nm ( $\epsilon = 5.9 \times 10^4 \text{ M}^{-1} \text{ cm}^{-1}$ ) and broad Q-like bands reaching into the NIR region (Figure 1).<sup>[8]</sup> The complex exhibited a parent-ion peak at  $m/z = 1520.8564$  ( $[M]^+$  calcd for C<sub>59</sub>H<sub>10</sub>F<sub>25</sub>N<sub>6</sub>O<sub>2</sub>Pd<sub>2</sub>: 1520.8529) in the HR mass spectrum, thus indicating the formation of a bispalladium complex, **4-Pd<sub>2</sub>**.

The structure of bispalladium complex **4-Pd<sub>2</sub>** was determined unambiguously by X-ray crystallographic analysis (Figure 2; see also Figure S13).<sup>[9]</sup> Two palladium cations reside within the macrocyclic NNNO cavities with square-planar geometry. The overall core structure of **4-Pd<sub>2</sub>** adopts a coplanar conformation. Both inner carbonyl groups are oriented toward the same side of the macrocyclic plane. The carbonyl oxygen atom located on the side of the

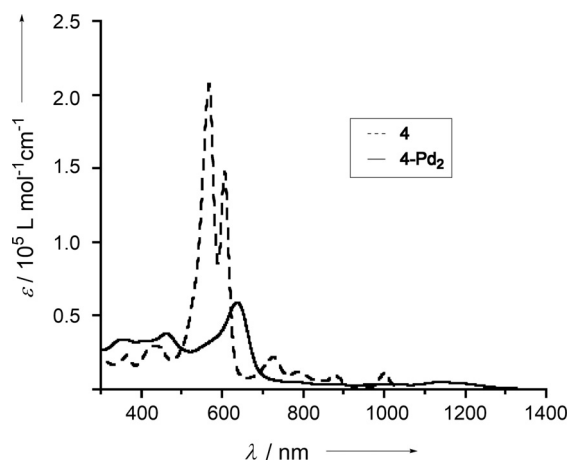


Figure 1. UV/Vis/NIR spectra of **4** and **4-Pd<sub>2</sub>** in CH<sub>2</sub>Cl<sub>2</sub>.

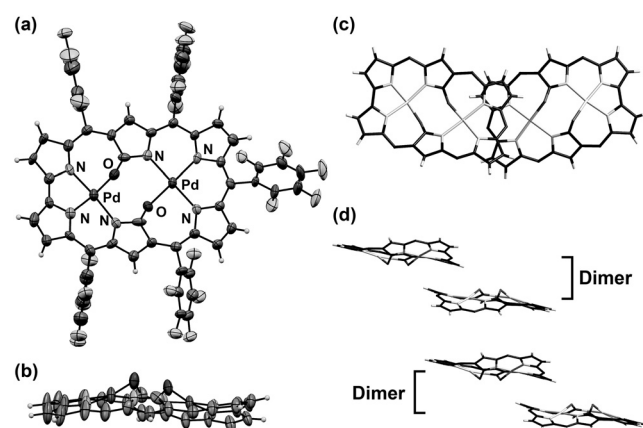


Figure 2. X-ray crystal structure of **4-Pd<sub>2</sub>** with thermal ellipsoids at 50% probability: a) top view, b) side view, and c, d) stacked dimeric structures. Solvent molecules and meso aryl groups are omitted for clarity in (b–d).

smaller coordination sphere deviates significantly from the mean plane of the macrocycle (mean deviation value defined by 35 atoms: 0.36 Å).

The bis-palladium complex **4-Pd<sub>2</sub>** demonstrated a unique paramagnetic character. The <sup>1</sup>H NMR spectrum of **4-Pd<sub>2</sub>** exhibited no resonance peaks in the usual diamagnetic region (−10–+15 ppm). Instead, an active electron paramagnetic resonance (EPR) signal at a *g*-tensor of 2.0021 was observed in toluene at 300 K (Figure 3a). The shape of the EPR signal of solid **4-Pd<sub>2</sub>** remained unchanged at a lower temperature (ca. 4 K; see Figure S14). Quantification of the amount of unpaired spin and the presence of no signals corresponding to  $\Delta m_s = \pm 2$  in the half-field region of **4-Pd<sub>2</sub>** suggested a typical organic monoradical ( $S = 1/2$ ) nature. In fact, unrestricted DFT (UB3LYP) calculations of the structure of **4-Pd<sub>2</sub>** reproduced the coplanar structure with an open-shell electronic character. The spin-density map of **4-Pd<sub>2</sub>** demonstrates that the unpaired electron is delocalized over the whole  $\pi$  framework of the hexaphyrin ligand, whereas marginal spin densities exist on both palladium centers (Mulliken spin density: 0.013951, 0.008796; Figure 3b). This

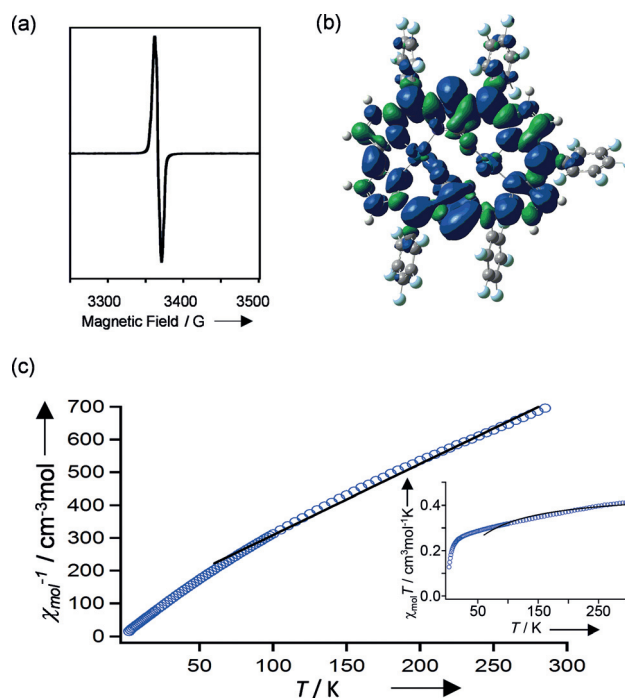
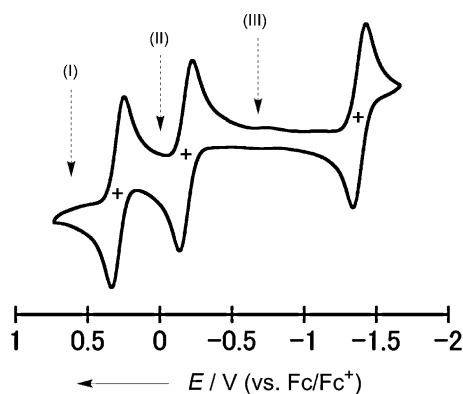


Figure 3. a) EPR spectrum of **4-Pd<sub>2</sub>** in toluene at 300 K. b) Spin-density map calculated at the UB3LYP/LANL2DZ and 6-31G\*\* level. c)  $\chi_{\text{mol}}^{-1}$ –*T* plot of solid **4-Pd<sub>2</sub>**, as determined by SQUID. Inset:  $\chi_{\text{mol}}^{-1}$ –*T* plot of solid **4-Pd<sub>2</sub>**.

result indicates the formation of an organic  $\pi$ -radicaloid species upon palladium complexation of the contracted [26]hexaphyrin **4**.

To examine the above rationale further, we determined the temperature-dependent magnetic susceptibility of solid **4-Pd<sub>2</sub>** by the use of a superconducting quantum interference device (SQUID; Figure 3c). The  $\chi_{\text{mol}}T$  value of **4-Pd<sub>2</sub>** recorded at room temperature is nearly identical to the theoretical index of 0.375 emu K mol<sup>−1</sup> expected for the doublet species.<sup>[10]</sup> The  $\chi_{\text{mol}}^{-1}$  value decreased gradually as the temperature was lowered. Fitting analysis of the  $\chi_{\text{mol}}^{-1}$  value in the range from 300 to 60 K by the use of the Curie–Weiss equation gave rise to a negative Weiss constant,  $\theta = -42.9$  K, which suggests the existence of an intermolecular antiferromagnetic interaction (see Figure S15). The crystal-packing structure of **4-Pd<sub>2</sub>** indeed revealed the formation of a weak  $\pi$ -stacking dimer with slipped parallel orientations (Figure 2d). The two interacting macrocyclic planes in the dimer have an intermolecular short atomic contact of 3.266 Å (see Figure S16), which is less than the sum of the van der Waals radii of two carbon atoms (3.4 Å).<sup>[11]</sup> This arrangement may arise from SOMO–SOMO overlap, despite the presence of the bulky meso pentafluorophenyl rings of **4-Pd<sub>2</sub>** (Figure 2c).

In an effort to determine the redox properties of **4-Pd<sub>2</sub>**, we carried out cyclic voltammetry in CH<sub>2</sub>Cl<sub>2</sub> containing 0.1 M *n*-tetrabutylammonium hexafluorophosphate as the electrolyte. A reversible one-electron oxidation wave at  $E_{\text{ox}} = 0.29$  V (versus ferrocene/ferrocenium) and two reversible one-electron reduction waves at  $E_{\text{red}} = -0.18$  and  $-1.38$  V were observed (Figure 4). These waves were assigned by spectro-



**Figure 4.** Cyclic voltammogram of **4-Pd<sub>2</sub>** in CH<sub>2</sub>Cl<sub>2</sub> containing 0.1 M *n*Bu<sub>4</sub>NPF<sub>6</sub>. Scan rate: 100 mV s<sup>-1</sup>. The cationic, neutral, and anionic states are assigned as states I–III, respectively.

electrochemical analysis of **4-Pd<sub>2</sub>**, whereby absorption spectra were obtained during electrochemical reaction in a thin-layered cell (see Figure S17). The original absorption spectrum of neutral **4-Pd<sub>2</sub>** (i.e., state II) was changed upon oxidation at 0.5 V. The spectrum of the product (i.e., state I) after the oxidation of **4-Pd<sub>2</sub>** exhibited a broad spectral feature with intense bands in the UV region, which could be interpreted according to a typical 4n  $\pi$ -electronic structure.<sup>[12]</sup> In contrast, a different pattern of spectral change was observed upon reduction at -0.5 V (state III): A Soret-like but broad band at  $\lambda_{\text{max}} = 677$  nm and relatively intense Q-bands with vibronic structures were observed in the NIR region. This spectral feature was reproduced by the chemical reduction of **4-Pd<sub>2</sub>** with decamethylferrocene (1 equiv; see Figure S18). Intriguingly, the absorption spectrum of the one-electron-reduced anionic product derived from **4-Pd<sub>2</sub>** resembles that of the bispalladium(II) doubly N-confused dioxo-[26]hexaphyrin **2-Pd<sub>2</sub>**, thus suggesting the regeneration of aromaticity in anionic **4-Pd<sub>2</sub>**.<sup>[13]</sup> The remarkably narrow HOMO–LUMO energy gap of 0.47 V could be rationalized by a significant anodic shift of the first reduction potential relative to the potentials of the free base **4**; first oxidation and reduction potentials of  $E_{\text{ox}} = 0.29$  V and  $E_{\text{red}} = -1.37$  V were found (see Figure S19 and Table S2). This result is consistent with the theoretical calculations. The marked stabilization of the  $\beta$ -spin LUMO of **4-Pd<sub>2</sub>** contributes to the narrow energy gap (see Figure S20).

In terms of the mechanism for the formation of the neutral radical **4-Pd<sub>2</sub>**, bispalladium complexation by the hexaphyrin ligand **4** leads to the open-shell doublet species. The hexaphyrin **4** offers unsymmetrical square-planar donor sites for palladium(II) cations. Considering that trivalent Pd (Pd<sup>III</sup>) complexes are rare, the potential Pd<sup>III</sup> complex could be unstable because it prefers to adopt a Jahn–Teller distorted-octahedral  $d^7$  electron configuration.<sup>[14]</sup> Therefore, the redox-noninnocent hexaphyrin backbone could enable one-electron transfer to the palladium centers to sustain square-planar Pd<sup>II</sup> complexes with an “NNNO” donor environment. As a result, the electronic state of **4-Pd<sub>2</sub>** is best considered as a neutral 25 $\pi$  electron conjugated radical species with non-aromaticity. The nearly zero NICS(0) value

of **4-Pd<sub>2</sub>** was estimated to be 2.6 ppm, which supports this conclusion (see Figure S22). In fact, this neutral radical species **4-Pd<sub>2</sub>** reveals significant chemical stability toward dioxygen as well as moisture (see Figure S23). The rigid and larger  $\pi$ -conjugated hexaphyrin scaffold could enable stabilization of the unpaired electron through delocalization over the macrocyclic circuit and kinetic blocking by the meso aryl groups.<sup>[3]</sup>

The third-order nonlinear optical (NLO) response of **4-Pd<sub>2</sub>** is also of interest in terms of the open-shell electronic structure, which gives rise to underlying static and dynamic polarizability.<sup>[15]</sup> The two-photon-absorption (TPA) cross-section value ( $\sigma^{(2)}$ ) of **4-Pd<sub>2</sub>** was determined by an open-aperture Z-scan method in the wavelength region ranging from 1500 to 2200 nm, in which one-photon absorption can be ignored (see Figure S24). The radical complex **4-Pd<sub>2</sub>** exhibited a maximum TPA cross-section value of 2100 GM upon photoexcitation at 1500 nm, whereas the closed-shell bispalladium(II) complex **2-Pd<sub>2</sub>** exhibited a maximum value of 900 GM at the same photoexcitation wavelength. The larger TPA cross-section value of **4-Pd<sub>2</sub>** might be attributed to its distinct spin-delocalized  $\pi$ -radical nature.

In conclusion, we have synthesized and characterized a novel skeletally contracted doubly N-confused hexaphyrin derivative **4**, which acts as a ligand for unsymmetrical metal coordination, that is, in the trianionic and dianionic NNNO cavities inside the macrocycle.<sup>[16]</sup> The bispalladium(II) complex **4-Pd<sub>2</sub>** showed a highly stable  $\pi$ -radical character identified by various spectroscopic and magnetometric means as well as theoretical calculations. The durability of the 25 $\pi$  neutral hexaphyrin radical **4-Pd<sub>2</sub>** under ambient conditions is notable and of scientific importance for the further extension of unsymmetrical-hexaphyrin-based coordination chemistry.

**Keywords:** expanded porphyrins · N-confusion · palladium · stable radicals · two-photon absorption

**How to cite:** *Angew. Chem. Int. Ed.* **2015**, *54*, 7323–7327  
*Angew. Chem.* **2015**, *127*, 7431–7435

- [1] a) J. L. Sessler, D. Seidel, *Angew. Chem. Int. Ed.* **2003**, *42*, 5134–5175; *Angew. Chem.* **2003**, *115*, 5292–5333; b) H. Furuta, H. Maeda, A. Osuka, *Chem. Commun.* **2002**, 1795–1804; c) S. Saito, A. Osuka, *Angew. Chem. Int. Ed.* **2011**, *50*, 4342–4373; *Angew. Chem.* **2011**, *123*, 4432–4464; d) M. Stępień, N. Sprutta, L. Latos-Grażyński, *Angew. Chem. Int. Ed.* **2011**, *50*, 4288–4340; *Angew. Chem.* **2011**, *123*, 4376–4430.
- [2] a) T. Koide, K. Youfu, S. Saito, A. Osuka, *Chem. Commun.* **2009**, 6047–6049; b) J. Sankar, S. Mori, S. Saito, H. Rath, M. Suzuki, Y. Inokuma, H. Shinokubo, K. S. Kim, Z. S. Yoon, J. Y. Shin, J. M. Lim, Y. Matsuzaki, O. Matsushita, A. Muranaka, N. Kobayashi, D. Kim, A. Osuka, *J. Am. Chem. Soc.* **2008**, *130*, 13568–13579.
- [3] a) T. Koide, G. Kashiwazaki, M. Suzuki, K. Furukawa, M. C. Yoon, S. Cho, D. Kim, A. Osuka, *Angew. Chem. Int. Ed.* **2008**, *47*, 9661–9665; *Angew. Chem.* **2008**, *120*, 9807–9811; b) T. Koide, K. Furukawa, H. Shinokubo, J. Shin, K. S. Kim, D. Kim, A. Osuka, *J. Am. Chem. Soc.* **2010**, *132*, 7246–7247; c) M. Ishida, S.-J. Kim, C. Prehls, K. Ohkubo, J. M. Lim, B. S. Lee, J. S. Park, V. M. Lynch, V. V. Roznyatovskiy, T. Sarma, P. K. Panda, C.-H. Lee, S. Fukuzumi, D. Kim, J. L. Sessler, *Nat. Chem.* **2013**, *5*, 15–20; d) L. K. Blusch, K. E. Craig, V. Martin-Diaconescu, A. B.



- McQuarters, E. Bill, S. Dechert, S. DeBeer, N. Lehnert, F. Meyer, *J. Am. Chem. Soc.* **2013**, *135*, 13892–13899; e) T. Y. Gopalakrishna, J. S. Reddy, V. G. Anand, *Angew. Chem. Int. Ed.* **2014**, *53*, 10984–10987; *Angew. Chem.* **2014**, *126*, 11164–11167.
- [4] a) S. Mori, A. Osuka, *J. Am. Chem. Soc.* **2005**, *127*, 8030–8031; b) Y. Tanaka, S. Saito, S. Mori, N. Aratani, H. Shinokubo, N. Shibata, Y. Higuchi, Z. S. Yoon, K. S. Kim, S. B. Noh, J. K. Park, D. Kim, A. Osuka, *Angew. Chem. Int. Ed.* **2008**, *47*, 681–684; *Angew. Chem.* **2008**, *120*, 693–696; c) S. Ishida, T. Tanaka, J. M. Lim, D. Kim, A. Osuka, *Chem. Eur. J.* **2014**, *20*, 8274–8278.
- [5] a) A. Srinivasan, T. Ishizuka, A. Osuka, H. Furuta, *J. Am. Chem. Soc.* **2003**, *125*, 878–879; b) I. Mayer, K. Nakamura, A. Srinivasan, H. Furuta, K. Araki, *J. Porphyrins Phthalocyanines* **2005**, *9*, 813–820; c) M. Suzuki, M.-C. Yoon, D. Y. Kim, J. H. Kwon, H. Furuta, D. Kim, A. Osuka, *Chem. Eur. J.* **2006**, *12*, 1754–1759; d) Y. Ikawa, M. Takeda, M. Suzuki, A. Osuka, H. Furuta, *Chem. Commun.* **2010**, *46*, 5689–5691.
- [6] S. Gokulnath, K. Yamaguchi, M. Toganoh, S. Mori, H. Uno, H. Furuta, *Angew. Chem. Int. Ed.* **2011**, *50*, 2302–2306; *Angew. Chem.* **2011**, *123*, 2350–2354.
- [7] A negligible amount of the product formed by monoacylation at the opposite  $\alpha$  position was detected. The regioselectivity of the acylation of **3** is discussed in the Supporting Information.
- [8] A lowest-energy transition at 1818 nm (0.68 eV,  $f=0.0002$ ) was predicted as an optically forbidden SOMO–1 to SOMO transition by a time-dependent (TD) DFT calculation according to the UB3LYP method (see Figure S21 and Table S3).
- [9] Two independent molecules were observed in the single crystal of **4-Pd**. One of them is shown in Figure 2. Crystal data for **4-Pd**, are provided in the Supporting Information. CCDC 1050934 contains the supplementary crystallographic data for this paper. These data can be obtained free of charge from The Cambridge Crystallographic Data Centre via [www.ccdc.cam.ac.uk/data\\_request/cif](http://www.ccdc.cam.ac.uk/data_request/cif).
- [10] In comparison with the theoretical value, the slight increase in the  $\chi_{\text{mol}} T$  value of **4-Pd**, presumably originated from partial, gradual vaporization of the solvent molecules present in the solid samples during the SQUID measurements.
- [11] A. Bondi, *J. Phys. Chem.* **1964**, *68*, 441–451.
- [12] S. Cho, Z. S. Yoon, K. S. Kim, M.-C. Yoon, D.-G. Cho, J. L. Sessler, D. Kim, *J. Phys. Chem. Lett.* **2010**, *1*, 895–900.
- [13] S. Gokulnath, K. Nishimura, M. Toganoh, S. Mori, H. Furuta, *Angew. Chem. Int. Ed.* **2013**, *52*, 6940–6943; *Angew. Chem.* **2013**, *125*, 7078–7081.
- [14] a) H. Furuta, H. Maeda, A. Osuka, M. Yasutake, T. Shinmyozu, Y. Ishikawa, *Chem. Commun.* **2000**, 1143–1144; b) L. M. Mirica, J. R. Khusnutdinova, *Coord. Chem. Rev.* **2013**, *257*, 299–314; c) K. J. Bonney, F. Schoenebeck, *Chem. Soc. Rev.* **2014**, *43*, 6609–6638.
- [15] M. Ishida, J. Shin, J. Lim, M. Yoon, T. Koide, J. L. Sessler, A. Osuka, D. Kim, *J. Am. Chem. Soc.* **2011**, *133*, 15533–15544.
- [16] The macrocycle **4** can be considered as a hybrid ligand system between a porphyrin and a corrole and is relevant to metallo-corrole chemistry with Group 10 elements (e.g., Ni), which stabilize open-shell low-spin  $d^8$  radical-cation states; see: a) S. Will, J. Lex, E. Vogel, H. Schmickler, J.-P. Gisselbrecht, C. Hubtmann, M. Bernard, M. Gross, *Angew. Chem. Int. Ed. Engl.* **1997**, *36*, 357–361; *Angew. Chem.* **1997**, *109*, 367–371; b) A. Ghosh, T. Wondimagegn, A. B. J. Parusel, *J. Am. Chem. Soc.* **2000**, *122*, 5100–5104.

Received: March 11, 2015

Published online: May 7, 2015